

INVESTIGATION ON EFFECT OF PROCESSING CONDITION ON PARTICLE DISPERSION IN CAST COMPONENT

Abstract

The processing of Metal Matrix Composites (MMCs) is widely carry out using liquid state processing route. Particle dispersion is the major concern while processing. The solidification influences dispersion of particles in cast condition. Subsequently, derive the change in mechanical and metallurgical properties of the material. A solidification rate is modify with the use of insulation on mold cavity. In literature, effect of processing condition i.e. insulation on properties of cast components of base metal or alloy were reported without considering metal composites. The aim of the current research is to investigate effect of insulation on particle dispersion in cast composites and to compare and analyse the results with the cast alloy. In the present investigation cube shape LM25/SiC composite (MMC) was developed using stir casting process. The solidification velocity (velocity of the solid-liquid interface) was calculated experimentally with the help of thermocouple, placed inside the mold cavity and associated data acquisition system. Critical velocity of the composite was calculated mathematically. Cube shape casting with two different processing condition were casted i.e. with and without insulation. Microstructure and hardness results were evaluated for the investigation of particle dispersion. From the present investigation it was observed that for LM25/SiC AMC, the solidification velocities above which engulfment occur was $0.087 \mu\text{m/s}$ with insulation and $0.117 \mu\text{m/s}$ without insulation. The microstructure images taken at different positions for two conditions reveal that the particles were pushed towards the grain boundaries, which confirms the result obtained from critical velocity calculation.

Keywords: Critical Velocity, Casting, Insulation, Particle Dispersion, Solidification Velocity

Authors

Vishal R. Mehta

Mechanical Engineering Department
Chandubhai S. Patel Institute of
Technology (CSPIT)
Faculty of Technology and
Engineering
Charotar University of Science and
Technology (CHARUSAT)
CHARUSAT- Campus, Changa 388
421, India
vishalmehta.me@charusat.ac.in

Mayur P. Sutaria

Mechanical Engineering Department
Chandubhai S. Patel Institute of
Technology (CSPIT)
Faculty of Technology and
Engineering
Charotar University of Science and
Technology (CHARUSAT)
CHARUSAT- Campus, Changa 388
421, India
mayursutaria.me@charusat.ac.in

I. INTRODUCTION

The foundry process is the most widely used practice for the processing of MMCs through liquid state processing route. The preliminary work on processing of cast composites was attempted by Badia and Rohatgi in 1965 [1]. In the subsequent years, processing of cast MMCs has shown significant progress for the applications in automotive industry [2-4]. Dwivedi et al., 2014 performed experimental investigation on microstructure and mechanical properties of LM25/SiC composites. They observed that with increase in the reinforcement contents i.e. 5, 10 and 15 wt.%, more SiC particles were present in the microstructure. The hardness values for LM25/SiC was found as 81.16 BHN, 92.33 BHN and 102 BHN for 5, 10 and 15 wt.% respectively [5]. Singh et al. 2017 have developed a stir casting setup and carried out experimentation using Al6063/SiC MMC with 10 wt% reinforcement content. Microstructure observation revealed uniform distribution of particles with presence of porosity [6]. The comprehensive research review on the development of MMCs through stir casting considering various factors has been presented by Ramanathan et al., 2019.

They have presented hardness of different Al alloy reinforced with SiC particles having various weight fraction of SiC. The value of brinell hardness ranges from 50 HB to 141 HB [7]. Surya and Gugulothu, 2022 have developed and characterized Al7075/SiC MMC. In their study they reported hardness of cast composites having SiC reinforcement content 5 wt.%, 10 wt.% and 15 wt.% as 83 BHN, 119 BHN and 124 BHN respectively. From the microstructure examination they reported uniform dispersion of particles with strong bonding between matrix and reinforcement particles and also reported that particle clustering increased with the increase in SiC content [8].

During solidification, the interaction between particles and matrix phase is influenced by the kinetic conditions evolve during liquid to solid transformation [9]. The kinetic conditions are governed by the critical velocity of the moving solid-liquid (S-L) interface. Particles are pushed ahead of S-L interface if solidification velocity is less than the critical value and get engulfed alternatively [10-13]. Recent reported research on solidification velocity are discussing behavior in alloy only i.e. not considering composites [14-17].

II. EXPERIMENTAL METHODOLOGY

In the present investigation cube shape composite having size of 90 mm x 90 mm was developed using optimum stirring parameters i.e. stirring speed of 400 rpm, stirrer position of 40 mm height and stirrer geometry (blade angle) 45 degree as per methodology adopted by the authors [18]. The cast composites having LM25 aluminium alloy as matrix material and 5 wt.% SiC particles as reinforcement was processed in the present investigation. The experiments were conducted with two different conditions such as, with and without use of insulating pad outside the mold cavity. The insulating pad having 20 mm thickness was used in the investigation. The solidification velocity (velocity of the solid-liquid interface) was calculated experimentally with the help of thermocouple, placed inside the mold cavity. The two cubes of aluminium alloy LM25 was casted having a configuration as with and without insulation along with two cube shape composite. The microstructure characterization and hardness testing of cast components were carried out to investigate particle dispersion.

To measure the temperature during solidification of the melt, thermocouples positions were as shown in Figure 1. The molds with insulating pad and thermocouples are shown in Figure 2. The temperatures at different locations were measured and recorded using National Instruments (NI) data acquisition system as shown in Figure 3.

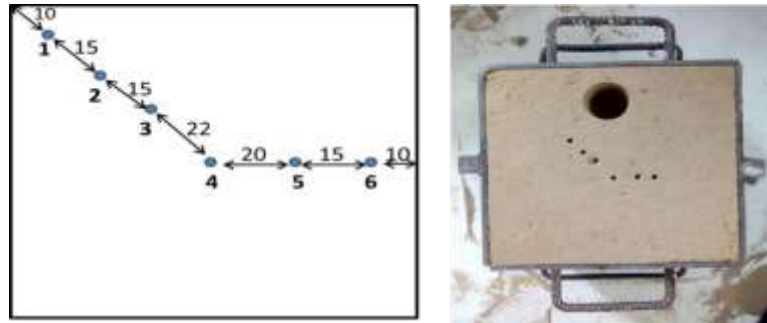


Figure 1: Locations of Thermocouples in Cube Shape Cavity (Dimentions are in mm)



Figure 2: Sand molds (a) With insulating pad and pattern (b) with insulating pad and thermocouples (c) without thermocouple and with insulating pad

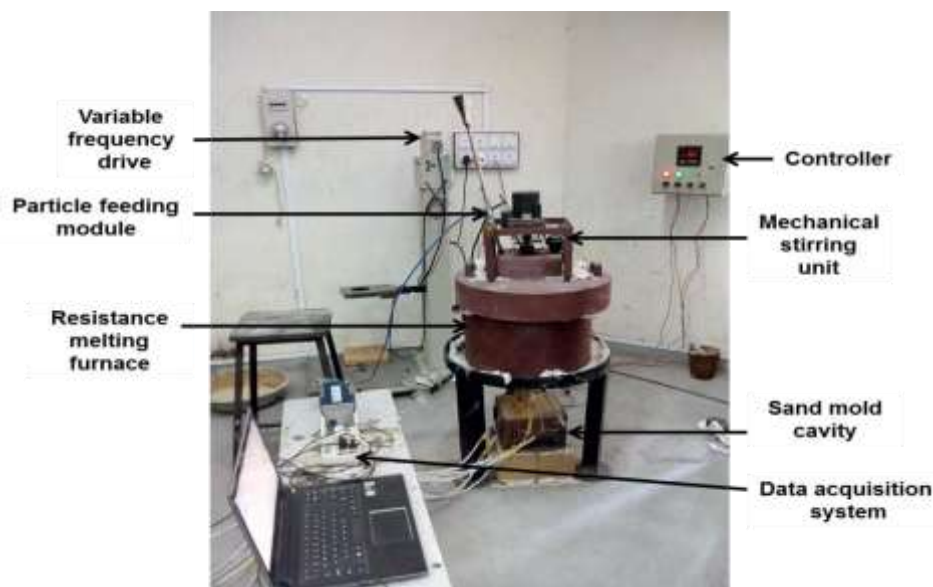


Figure 3: Experimental setup with the data acquisition system

- 1. Solidification Velocity:** In order to find out solidification velocity of cube casting, the temperature at various locations as shown in Figure 1 were measured using k-type thermocouples. The one end of the k-type thermocouple was inserted in the mold up to parting line of the cavity and other ends were connected to the temperature input module NI TB9214 of NI data acquisition system as shown in Figure 3. The data acquisition system is equipped with LabView signal express software, which measures and record the temperature at an interval of 0.5 seconds. The time for solidification at the particular location was evaluated from data obtained through the data acquisition system. The solidification velocity was calculated from the relation proposed by [9] as mentioned in Equation 1. The research work reported by [9] presents latest reported work for the composites, other recent research works focus on pure metal or alloy only. Hence, their work is considered as reference for the present study.

$$V = \frac{d_{avg}}{8t_s} \quad (1)$$

Where, d_{avg} = Average diameter of particle
 t_s = Solidification time

The average diameter of particle (d_{avg}) was measured from the micrographs using Biovis MP image analysis software. The solidification velocities at different locations for LM25/SiC MMC with and without insulation are presented in Table 1 and 2 respectively.

Table 1: Solidification velocities of LM25/SiC composite with insulation

Locations	V1 (1-2)	V2 (2-3)	V3 (3-4)	V4 (4-5)	V5 (5-6)	Average
Solidification Velocities ($\mu\text{m/s}$)	0.196	0.014	0.022	0.021	0.183	0.087

Table 2: Solidification velocities of LM25/SiC composite without insulation

Locations	V1' (1-2)	V2' (2-3)	V3' (3-4)	V4' (4-5)	V5' (5-6)	Average
Solidification Velocities ($\mu\text{m/s}$)	0.224	0.031	0.067	0.067	0.193	0.117

- 2. Critical Velocity:** During solidification, the interaction between particles and matrix phase is influenced by the kinetic conditions evolve during liquid to solid transformation [10]. The kinetic conditions are governed by the critical velocity of the moving solid-liquid (S-L) interface. Particles are pushed ahead of S-L interface if solidification velocity is less than the critical value and get engulfed alternatively [12].

The critical velocity in the present investigation was calculated using the analytical model presented by [9]. They have presented an analytical equation of the critical velocity as mentioned in Equation 2.

$$V_c = \left(\frac{1}{6} \frac{B}{\eta h^2} \left(1 + e^{\pi^2 \left(1 - \frac{r}{cr} \right)} \right) \right)^{-1} \quad (2)$$

Where, V_c = Critical velocity in $\mu\text{m}/\text{sec}$

B = Hamaker constant between particle and interface

h = Minimum separation distance between particle and interface = 1×10^{-8} m

η = Viscosity of the melt

r = Particle radius

cr = Critical radius of the particle

The critical radius of the particle is evaluated from Equation 3 as shown below.

$$cr = \left(\frac{27}{4} \frac{K_b T \eta}{\pi \Delta t (\rho_p - \rho_l^2) g^2} \right)^{\frac{1}{5}} \quad (3)$$

Where, ρ_p = Density of SiC particle

ρ_l = Density of Al alloy melt g = Gravitational acceleration K_b = Boltzmann constant

T = Absolute temperature of the metal

Δt = The time interval of action of the Brownian force

The parameters used for calculations of critical velocities in LM25/SiC system are presented in Table 3. The critical velocity was obtained as $4.158 \mu\text{m}/\text{s}$, according to Equation 2.

Table 3: Parameters used for calculation of critical velocity in Al-SiC system

Parameter	Value	Unit	Reference
B	1×10^{-21}	Unit less	[19]
h	1×10^{-8}	m	[9]
η	0.4	Pa.s	[20]
r	22	μm	Calculated
ρ_p	3200	kg/m^3	Material Property
ρ_l	2700	kg/m^3	Material Property
g	9.8	m/s^2	Constant
K_b	1.38×10^{-23}	J/K	[9]
T	923	K	Material Property
Δt	1×10^{-3}	S	[21]

- 3. Hardness Testing:** In order to investigate the effect of processing conditions and mold cavity on the dispersion of reinforcement particles hardness testing of cast components was carried out using hardness tester as shown in Figure 4. The Brinell Hardness Number (BHN) was measured along the diagonal direction of cast components at an interval of 15 mm as shown in

Figure 5 (dimensions are in mm). The BHN was measured for the total four cube casting, i.e. cube casting of LM25 with and without insulating pad; and cube casting of LM25/SiC MMC with and without insulating pad.



Figure 4: Hardness tester used for Brinell hardness number measurement

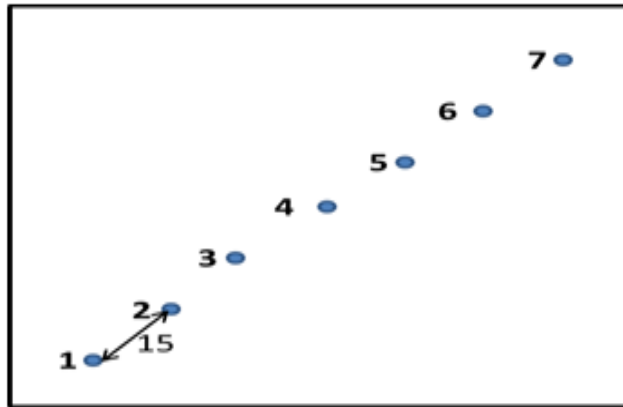


Figure 5: Locations for Brinell hardness number measurement

The hardness value (BHN) measured for LM25/SiC composites at two different processing conditions are presented in Table 4. The hardness value of aluminium alloy LM25 was evaluated in a similar manner. The mean hardness value of LM25 has been evaluated as 125 and 135 BHN for with and without insulation respectively.

Table 4: Hardness value of LM25/SiC MMC for different processing condition

Locations	Distance (mm)	Without Insulation	With Insulation
1	15	131	135
2	30	132	137
3	45	133	138
4	60	135	146
5	75	136	147
6	90	133	139
7	105	130	134
Average BHN		132.86	139.43

4. Microstructure Characterization: The effect of processing condition on the dispersion of particles inside the mold cavity was evaluated by the microstructure analysis of cube casting. The microstructural analysis was carried out using the Zeiss Axiovert metallurgical microscope equipped with Biovis MP software for image analysis. The specimens were prepared for metallographic examinations using 120–220–400–600–800 mesh emery papers, followed by polishing with alumina paste. Keller’s reagent was used for etching of the samples. The microstructure images of aluminium alloy LM25 with and without insulation are shown in Figure 6. The cube casting was sectioned into three different pieces, i.e. top, middle and bottom for the two processing condition with and without insulation. The samples from these pieces were analyzed for microstructure testing and images of microstructure are presented in Figure7.

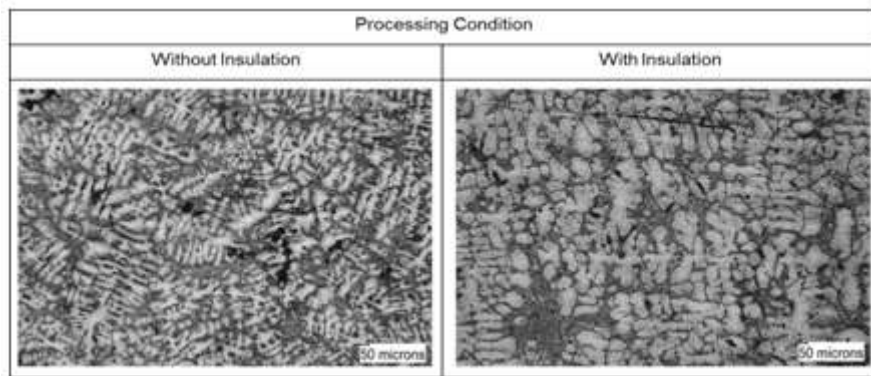


Figure 6: Microstructure images of Al alloy LM25 for two different processing conditions

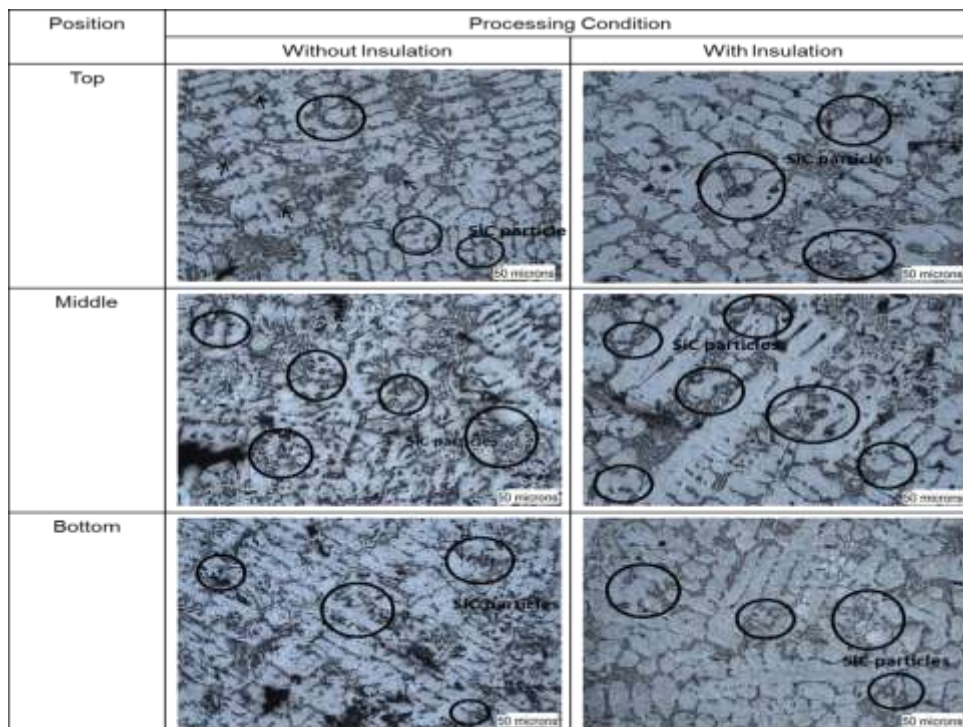


Figure 7: Microstructure images of LM25/SiC composite at different positions for two different processing conditions

5. Effect of Processing Condition on Particle Dispersion: The solidification of composite slurry involves the interaction between solid-liquid (S-L) interface and suspended reinforcement particles, which influence the particle dispersion. The particles are either engulfed by the S-L interface, resulting in the dispersion of particle within the grain; or S-L interface pushes the particles towards grain boundaries and eutectic region. Particles are pushed ahead of S-L interface if solidification velocity is less than the critical value and get engulfed alternatively [22].

The solidification velocity of LM25/SiC composite for two processing condition viz. with and without insulation has been evaluated and presented in Table 1 and 2 respectively. The solidification velocities of the composite with insulation were lower than the composite without use of insulation for all the locations. The critical velocity of LM25/SiC system was calculated as $4.158 \mu\text{m/s}$. The solidification velocities for both the processing condition and for all the locations were lower than the critical velocity resulting in particle pushing. The solidification velocities above which engulfment occur was found to be $0.087 \mu\text{m/s}$ and $0.117 \mu\text{m/s}$ for LM25/SiC with and without insulation respectively.

The microstructure images taken at different positions for two different conditions reveal that the particles were pushed towards the grain boundaries, which confirms the result obtained from critical velocity calculation. The higher dendrite arm spacing was observed in the micrographs of cast composite with insulation as compared without insulation.

The hardness number distribution along the diagonal of the specimen for two different processing conditions is shown in Figure 8. The higher value of hardness has been observed for a specimen with insulation along the diagonal direction of the specimen. The low hardness number was observed for the area near corners of the specimen and for area near the center of the specimen higher hardness number was observed due to interaction of the solid-liquid (S-L) interface. The hardness values (BHN) of LM25/SiC composites were 13.63% and 8.22% higher than the LM25 alloy for with and without insulation, respectively. The use of insulation around mold cavity for composite increased the hardness by 12.95% compared to without provision of insulation.

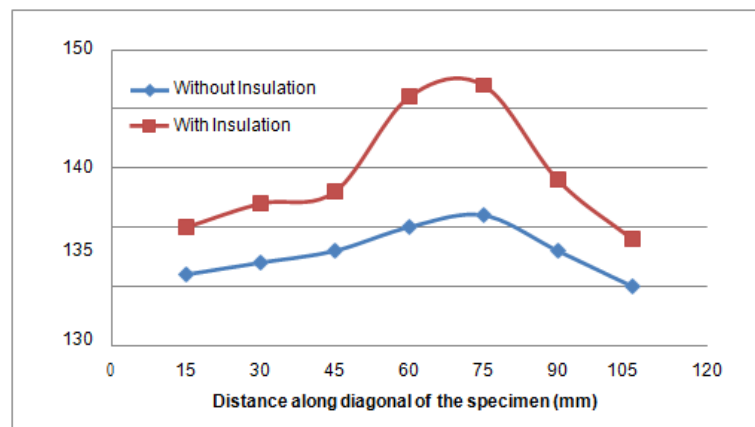


Figure 8: Effect of processing condition on hardness of Al-SiC MMC

III. CONCLUSIONS

- The solidification velocities above which engulfment occur was found to be 0.087 $\mu\text{m/s}$ and 0.117 $\mu\text{m/s}$ for LM25/SiC with and without insulation respectively.
- The microstructure of composite sample taken at different positions for two different conditions reveal that the particles were pushed towards the grain boundaries, which confirms the result obtained from critical velocity calculation.
- The low hardness number was observed for the area near corners of the specimen and for area near the center of the specimen higher hardness number was observed due to interaction of the solid-liquid (S-L) interface.
- The hardness values (BHN) of LM25/SiC composites were 13.63% and 8.22% higher than the LM25 alloy for with and without insulation, respectively.
- The use of insulation around mold cavity for composite increased the hardness by 12.95% compared to without provision of insulation.

REFERENCES

- [1] F.A. Badia, P.K. Rohatgi, Dispersion of graphite particles in aluminum castings through injection of the melt. *Trans. AFS* 76, 402–406 (1969).
- [2] V. S. Ayar, M. P. Sutaria, Comparative evaluation of ex situ and in situ method of fabricating aluminum/TiB₂ composites. *International Journal of Metal Casting*, 15, 1047–1056 (2021). <https://doi.org/10.1007/s40962-020-00539-7>
- [3] Ajay Kumar, P., P. Rohatgi, D. Weiss, 50 years of foundry-produced metal matrix composites and future opportunities. *International Journal of Metal Casting*, 14(2), 291-317 (2020). <https://doi.org/10.1007/s40962-019-00375-4>
- [4] J. M. Mistry, P. P. Gohil, Research review of diversified reinforcement on aluminum metal matrix composites: fabrication processes and mechanical characterization. *Science and Engineering of Composite Materials*, 25(4), 633-647 (2018). <https://doi.org/10.1515/secm-2016-0278>
- [5] S. P. Dwivedi, S. Sharma, R. K. Mishra, Comparison of microstructure and mechanical properties of A356/SiC metal matrix composites produced by two different melting routes. *International Journal of Manufacturing Engineering*, (2014). <http://dx.doi.org/10.1155/2014/747865>
- [6] S. Singh, I. Singh, A. Dwivedi, Design and development of novel cost effective casting route for production of metal matrix composites (MMCs). *International Journal of Cast Metals Research*, 30(6), 356-364 (2017). <https://doi.org/10.1080/13640461.2017.1323605>
- [7] A. Ramanathan, P. K. Krishnan, R. Muraliraja, A review on the production of metal matrix composites through stir casting–Furnace design, properties, challenges, and research opportunities. *Journal of Manufacturing processes*, 42, 213-245 (2019). <https://doi.org/10.1016/j.jmapro.2019.04.017>
- [8] M. S. Surya, S. K. Gugulothu, Fabrication, mechanical and wear characterization of silicon carbide reinforced Aluminium 7075 metal matrix composite. *Silicon*, 14(5), 2023-2032 (2022). <https://doi.org/10.1007/s12633-021-00992-x>
- [9] X. H. Chen, H. Yan, Solid–liquid interface dynamics during solidification of Al 7075–Al₂O₃np based metal matrix composites. *Materials & Design*, 94, 148-158 (2016). <https://doi.org/10.1016/j.matdes.2016.01.042>
- [10] J.B. Ferguson, G. Kaptay, B.F. Schultz, P.K. Rohatgi, K. Cho, C.S.Kim, Brownian motion effects on particle pushing and engulfment during solidification in metal-matrix composites. *Metallurgical and Materials Transactions A*, 45(10), 4635–4645 (2014). <https://doi.org/10.1007/s11661-014-2379-x>.
- [11] E.M. Agalotis, C.E. Schvezov, M.R. Rosenberger, A.E. Ares, A numerical model study of the effect of interface shape on particle pushing. *Journal of Crystal Growth*, 354(1), 49–56 (2012). <https://doi.org/10.1016/j.jcrysgro.2012.05.032>
- [12] S. Karagadde, S. Sundarraj, P. Dutta, A model for growth and engulfment of gas microporosity during aluminum alloy solidification process. *Computational materials science*, 65, 383–394 (2012). <https://doi.org/10.1016/j.commatsci.2012.07.045>

- [13] P.K. Rohatgi, K. Pasciak, C.S. Narendranath, S. Ray, A. Sachdev, Evolution of microstructure and local thermal conditions during directional solidification of LM25-SiC particle composites. *Journal of materials science*, 29(20), 5357–5366 (1994). <https://doi.org/10.1007/BF01171548>
- [14] J.E. Rodriguez, C. Kreisler, T. Volkmann, D. M. Matson, Solidification velocity of undercooled Fe–Co alloys. *Acta Materialia*, 122, 431-437 (2017). <https://doi.org/10.1016/j.actamat.2016.09.047>
- [15] H. Zheng, R. Chen, G. Qin, X. Li, Y. Su, H. Ding, J. Guo, and H. Fu, Transition of solid-liquid interface and tensile properties of CoCrFeNi high-entropy alloys during directional solidification. *Journal of Alloys and Compounds*, 787, 1023-1031 (2019). <https://doi.org/10.1016/j.jallcom.2019.02.050>
- [16] V. Bathula, C. Liu, K. Zwiack, J. McKeown, J. M. Wiezorek, Interface velocity dependent solute trapping and phase selection during rapid solidification of laser melted hypo-eutectic Al-11at.% Cu alloy. *Acta Materialia*, 195, 341-357 (2020). <https://doi.org/10.1016/j.actamat.2020.04.006>
- [17] Y. An, X. Xu, Y. Hao, R. Dong, H. Hou, Y. Zhao, T. Gu, and H. Wang, Effect of Co addition on solidification velocity, hardness and refined structure transformation mechanisms of undercooled Ni-Cu-Co alloys. *Journal of Alloys and Compounds*, 921, 166150 (2022). <https://doi.org/10.1016/j.jallcom.2022.166150>
- [18] V. R. Mehta, M. P. Sutaria, Investigation on the effect of stirring process parameters on the dispersion of SiC particles inside melting crucible. *Metals and Materials International*, 27(8), 2989-3002 (2021). <https://doi.org/10.1007/s12540-020-00612-0>
- [19] Y.M. Youssef, R.J. Dashwood, P.D. Lee, Effect of clustering on particle pushing and solidification behaviour in TiB₂ reinforced aluminium PMMCs. *Composites Part A: Applied Science and Manufacturing*, 36(6):747- 63 (2005). <https://doi.org/10.1016/j.compositesa.2004.10.027>
- [20] J. Dutkiewicz, H.V. Atkinson, L. Lityńska-Dobrzyńska, T. Czeppe, M. Modigell, Characterization of semi- solid processing of aluminium alloy 7075 with Sc and Zr additions. *Materials Science and Engineering: A.*, 580:362-73 (2013). <https://doi.org/10.1016/j.msea.2013.04.078>
- [21] M. Sato, H. Katsuno, Y. Suzuki, Ordering of Brownian particles from walls due to an external force. *Journal of Crystal Growth*, 401:87-92 (2014). <https://doi.org/10.1016/j.jcrysgro.2014.01.074>
- [22] J. W. Garvin, Y. Yang, H. S. Udaykumar, Multiscale modeling of particle–solidification front dynamics, Part I: Methodology. *International journal of heat and mass transfer*, 50 (15-16), 2952-2968 (2007). <https://doi.org/10.1016/j.ijheatmasstransfer.2006.12.031>